New Trends in Thermal Neutron Spectrometry Getting High-Resolution Performances in Thermal Neutrons Spectrometry by Using Inverse Space Focusing

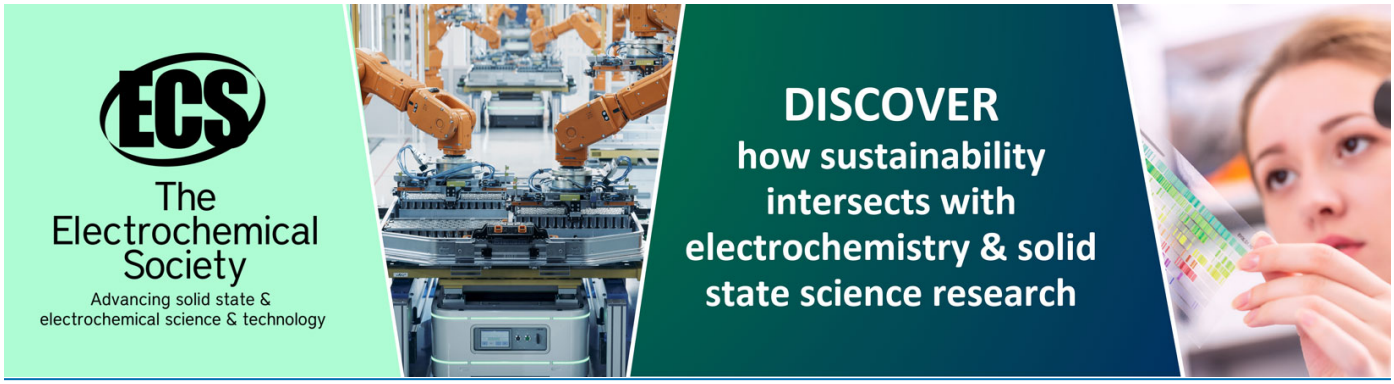

New Trends in Thermal Neutron Spectrometry Getting High-Resolution Performances in Thermal Neutrons Spectrometry by Using Inverse Space Focusing

I. Ionita, C. Paunoiu, V. Florescu
Institute for Nuclear Research Pitesti
ICN Pitesti, Campului Street No. 1, Pitesti – Mioveni, Arges, Romania

E-mail: ionionita@lycos.com, cpaunoiu@email.com, valeriu.florescu@nuclear.ro

Abstract. The characteristics of a Q-space focusing configuration are given. The procedure to get inverse space conditions is given also. Both the diffraction and inelastic scattering are considered. For the neutron diffractometry both instruments with one crystal monochromator and with two crystals monochromators are taken into consideration. The time of flight diffractometers both for a pulsed neutron source and a steady state one is considered also. For inelastic scattering the inverse space focusing conditions for triple axis spectrometers are givene line-width.

Introduction

In neutron spectrometry the optimal use of the available neutrons is of the greatest importance. The general philosophy to do it is to maximize the neutron flux at sample by using neutron guides, supermirrors [1], or spatial focusing effects involving flexible configurations and curved crystals. A different approach [2], [3], is to obtain the required optimum experimental conditions not by getting focused beams at sample or anywhere else, but only by decreasing as much as possible the scan variable variances.

A Q-space focussing configuration is characterized by high-resolution even when no spatial focussing exist at sample position or anywhere else or is used quite open beam without any Soller collimators; only coarse collimators should be used to reduce the background level.

This is possible just by decreasing the scan variable variances.

The following steps should be followed:

- to define the scan variable
- to define the significant spatial variables as are the monochromator and sample width for example
- to express the scan variable, using specific geometry characteristics and the existing correlation between variables, through the spatial variables
- to cancel the significant contributions to the scans variable variances by cancelling the important variables coefficients, from the scan variable expression; *when correlation between variable exists*, as is the case for these kind of experimental configurations, such a coefficient has more then one term, not all of the same sign, appearing the possibility to be cancelled and therefore to cancel entirely the corresponding contribution of this spatial variable to the line-width.

Examples for neutron diffractometers and triple axis spectrometer are given bellow.

Neutron Diffractometers

2.1. The General Method

In the neutron diffractometry the scan variable is X_1, the X vector component along the Q_0 direction, where $X=Q-Q_0$ and $Q = k_f-k_i$; k_f, k_i are the wave vectors for the incoming respectively the diffracted neutrons and "0" refers to the corresponding most probable value. The scan variable is given by:

$$X_1 = 2 \cdot \Delta k \cdot \sin\theta_s + k \cdot (\gamma_f - \gamma_i) \tag{1}$$

where γ_I ,γ_f are the horizontal divergence angles from the most probable trajectories, Δk is the wave vector spread, $2\theta_s$ is the scattering angle; the indices i,f refer to the incoming respectively the scattered neutrons. The variables defining the neutron trajectories in phase space are all the spatial relevant coordinates to which has to be added, for the time-of-flight diffractometry, the temporal variables defining its emission respectively detection. All the spatial and temporal variables are measured from the corresponding most probable values. The relation defining the temporal variables is:

$$\frac{h}{2\pi m} \cdot (t_f - t_0) = \frac{\Delta L}{k} - \frac{L}{k} \cdot \frac{\Delta k}{k} \tag{2}$$

where L is the neutron flight path from source (from chopper centre for a steady state source) to detector, h is the Plank constant and m is the neutron mass.

For the crystal diffractometry the Bragg constraints have to be considered:

$$\left.\begin{aligned} \gamma_i - \gamma_f &= 2 \cdot \frac{l_m}{R_m} \cdot sign(\theta_m + \chi_m) \\ \frac{\Delta k}{k} &= \cot\theta_m \cdot \frac{\gamma_i - \gamma_f}{2} \end{aligned}\right\} \tag{3}$$

The relation (2) and (3) defines the Δk in (1) for the time-of-flight respectively the crystal diffractometry. To these relations must be added the relations giving the horizontal angular variables expressed through the spatial variables l_0, l_s,, l_d, , l_m the source, sample, detector and monochromator lengths; R_m is the crystal radius of curvature. The general procedure is to express the scan variable X_1 through spatial and, for time-of-flight diffractometry, temporal variables and to cancel the major contributions, i.e. the l_0, l_s,, l_d, , l_m coefficients.

2.2. The Crystal Diffractometry

2.2.1. One Crystal Monochromator

For this geometry (see Figure 1), following the above-described procedure and cancelling the l_m coefficient, one obtains:

$$R_m = \frac{2a}{2a-1} \cdot \frac{L \cdot sign(\theta_m + \chi_m)}{\sin(\theta_m - \chi_m)} \tag{4}$$

where

$$a = -\tan\theta_s / \tan\theta_m$$

$$\mathrm{sign}\alpha = \mathrm{abs}\alpha / \alpha$$

Cancelling the "l_s" coefficient one obtains:

$$\left.\begin{aligned} \tan\chi_s &= \cot\theta_s \cdot [1 - \frac{2}{1+(2a-1)\cdot\frac{L_2}{L_1}}] \\ \cot\alpha_s &= \frac{\cos(2\theta_s) - (2a-1)\cdot\frac{L_2}{L_1}}{\sin(2\theta_s)} \\ \alpha_s &= \chi_s + \theta_s + \pi/2 \end{aligned}\right\} \quad (5)$$

where α_s as the inclination angle measured from the monochromatic beam direction.

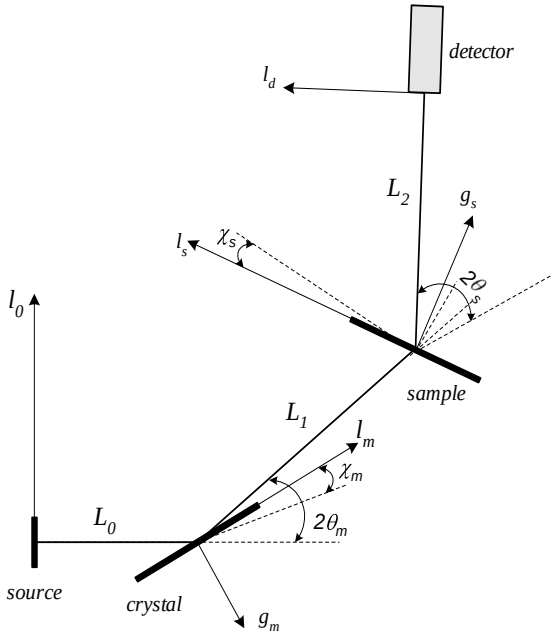

Figure 1

The (5) condition is fulfilled if the sample is rotated during the experimental diffraction pattern raising; for each value of the scattering angle the sample has to be positioned accordingly to the (5) relation. In this case the contribution to the line-width of the sample width is cancelled. But, as in this situation, the sample effective volume where the neutrons are scattered, is different for each value of the scattering angle, the normal Rietveld experimental data processing procedure should be modified accordingly.

The (4) relation is the condition to cancel the monochromator width contribution to the line-width. But as the crystal reflectivity is strongly dependent on the radius of curvature, is not possible to be changed during the diffraction pattern raising; this would lead to a significant variation of the incident beam intensity and no data processing is possible in this situation. It is convenient to keep the monochromator radius of curvature constant, at a value corresponding to that given by (4) for a scattering angle $2\theta_s$ in the range 90-110 degrees, where the overlapping problems are the most significant and therefore the line-width should be minimum. A value of around 10 m for the monochromator radius of curvature is quite convenient, giving a minimum line-width of 12-15 minutes and not more than 25 minutes for the rest of scattering angle values.

An important problem appears. The sample position given by (5) correspond to a certain value of the scattering angle $2\theta_s$. The question is: if we keep the same sample position corresponding to a certain scattering angle value, how much is decreased the resolution if we measure the pattern for a certain

angular range, around this value? Can be used a position sensitive detector in the case of Q-space focussing configurations?
To find an answer to this important problem, computations were made, using the DAX program [4], for the configuration existing at INR Pitesti and a sample of 2.5 cm width, 3 cm height and .5 cm thickness, for 5 values of the scattering angle, 30^0, 50^0, 70^0, 90^0 and 110^0, for which the optimum sample orientation angles are 29^0, 37^0, 90^0, 121^0, 144^0 respectively; were computed the line widths for a range of 20^0 around the above mentioned scattering angle values. The results are given in Figure 2.

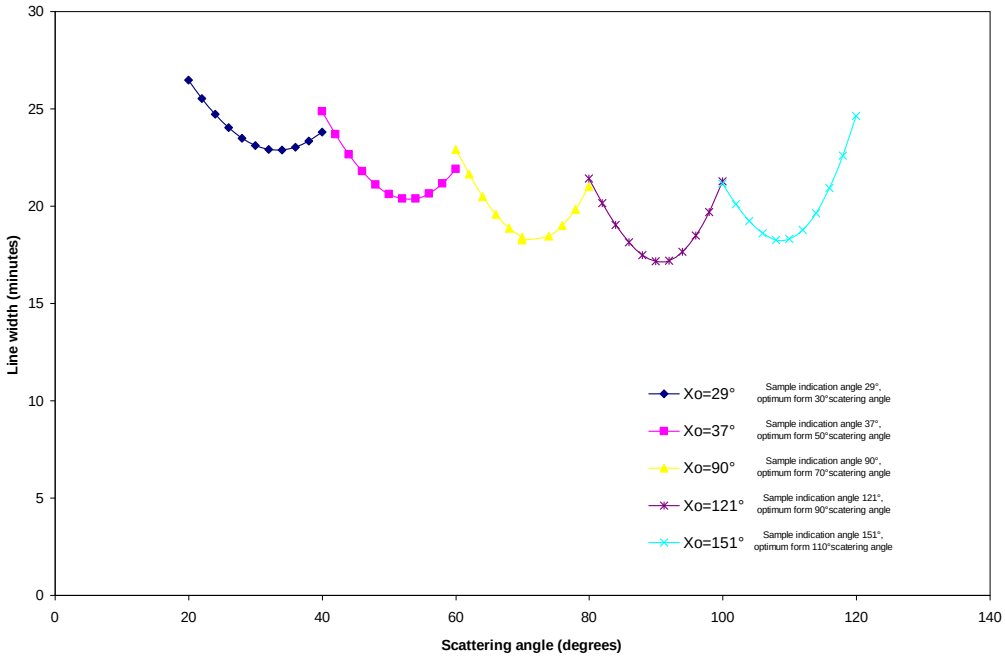

Figure 2

The conclusion is quite obvious: the resolution is still very good even for a range of 20^0 around the scattering angle for which the sample is in the optimum position; if still a better resolution is desired, the detector angular width can be lowered at 15^0; that means that the diffraction pattern can be got from 5 -7 steps.
Considering the advantages offered by a Q-space focussing configuration in comparison with the high resolution conventional ones, we have to mention that the neutrons use efficiency is better with a factor of $10^3/5$, were 10^3 is roughly the transmission of the Soller collimators system defining the conventional instrument considered; that means that with a lower flux of two order of magnitude can be obtained the same luminosity (the same measure time); for comparable neutrons flux the measure time can be reduced correspondingly.

2.2.2. Two Crystals Monochromator

For this geometry (see Figure 3), following the above-described procedure, tacking account that the Bragg constraints, for the two crystals, are:

$$\left.\begin{aligned}\gamma_0+\gamma_1 &= 2\cdot sign(\theta_{m1}+\chi_{m1})\cdot\frac{l_{m1}}{R_{m1}}\\ \gamma_2+\gamma_1 &= 2\cdot sign(\theta_{m2}+\chi_{m2})\cdot\frac{l_{m2}}{R_{m2}}\end{aligned}\right\} \qquad (6)$$

$$\left.\begin{aligned}\frac{\Delta k_1}{k} &= (\gamma_0 - \gamma_1)\cdot\frac{\cot\theta_{m1}}{2}\\ \frac{\Delta k_2}{k} &= (\gamma_1 - \gamma_2)\cdot\frac{\cot\theta_{m21}}{2}\end{aligned}\right\} \tag{7}$$

to which it has to be added the condition that the neutrons reflected by the first crystal must have a proper wave-length to be reflected by the second crystal, i.e.

$$\left.\begin{aligned}&\Delta k_i = \Delta k_f\\ &or\\ &\gamma_2 = \gamma_1\cdot\ 1-\mathrm{a_m}\ +\mathrm{a_m}\cdot\gamma_0\end{aligned}\right\} \tag{8}$$

with $a_m = \tan\theta_{m2} / \tan\theta_{m1}$.

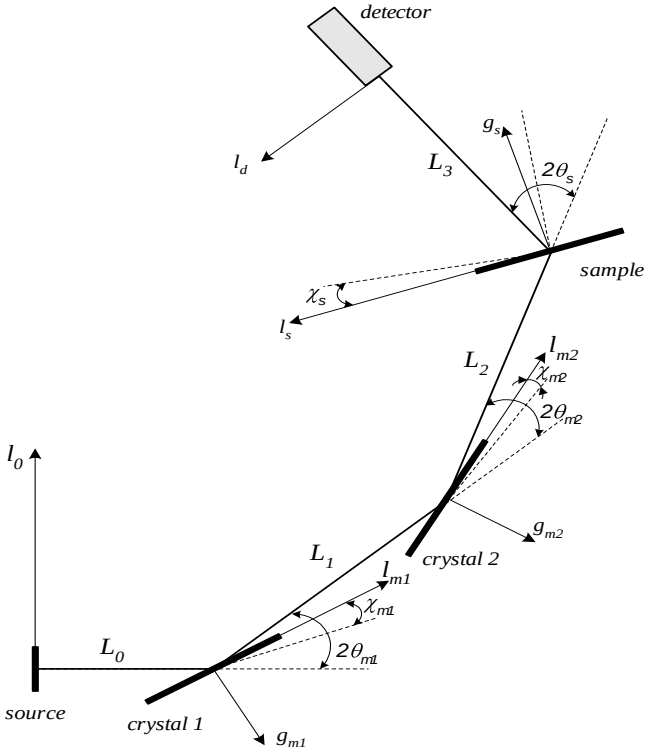

Figure 3

One obtains the following focusing conditions, giving the crystals radii of curvature:

$$\left.\begin{aligned}\frac{1}{R_1} &= \frac{a_m - 1}{a_m\cdot L_1}\cdot sign(\theta_{m1} + \chi_{m1})\cdot\sin(\theta_{m1} - \chi_{m1})\\ \frac{1}{R_2} &= -\frac{a_m - 1}{L_1}\cdot sign(\theta_{m2} + \chi_{m2})\cdot\sin(\theta_{m2} + \chi_{m2})\end{aligned}\right\} \tag{9}$$

By cancelling the "l_0" and "l_s" coefficients, one obtains respectively

$$\left.\begin{aligned} \frac{L_2}{L_1} &= \frac{1+\frac{a_m}{2a}}{1-a_m}\cdot\frac{\sin(\theta_{m2}-\chi_{m2})}{\sin(\theta_{m1}+\chi_{m1})} \\ \tan\chi_s &= \cot\theta_s\cdot\frac{\xi-1}{\xi+1} \end{aligned}\right\} \tag{10}$$

with

$$\left.\begin{aligned} \xi &= -\frac{L_3}{L_2}\cdot\frac{2\cdot(a+a_m)-1-2\cdot\alpha_1\cdot(1-\frac{1}{a_m})\cdot(a+a_m-1)}{2a_m-1-2\cdot\alpha_1\cdot\frac{(1-a_m)^2}{a_m}+\alpha_2\cdot(1+\alpha_1\cdot\frac{2-a_m}{a_m})} \\ \alpha_1 &= \frac{L_0}{L_1}\cdot\frac{\sin(\theta_{m1}-\chi_{m1})}{\sin(\theta_{m1}+\chi_{m1})},\quad \alpha_2 = \frac{L_2}{L_1}\cdot\frac{\sin(\theta_{m2}-\chi_{m2})}{\sin(\theta_{m2}+\chi_{m2})} \end{aligned}\right\} \tag{11}$$

2.3. The Time-of-Flight Diffractometry

2.3.1. Pulsed Source

For this geometry (see Figure 4) following the above-described procedure, tacking account that

$$L = L_0 + L_1$$

$$\Delta L = -l_d\cdot\sin\chi_d - 2\cdot l_s\cdot\sin\theta_s\cdot\cos\chi_s + l_0\cdot\sin\chi_0,$$

by cancelling the "l_d", "l_s" and "l_0" coefficients, one obtains, respectively:

$$\left.\begin{aligned} \tan\chi_d &= \cot\theta_s\cdot\frac{L}{2\cdot L_1} \\ \tan\chi_s &= \frac{\frac{4\cdot\tan^2\theta_s}{L}+\frac{1}{L_1}+\frac{1}{L_0}}{\tan\theta_s\cdot(\frac{1}{L_0}-\frac{1}{L_1})} \\ \tan\chi_0 &= -\cot\theta_s\cdot\frac{L}{2\cdot L_0} \end{aligned}\right\} \tag{12}$$

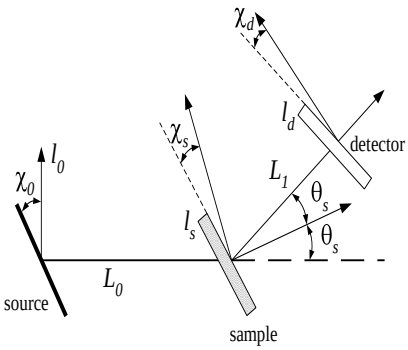

Figure 4

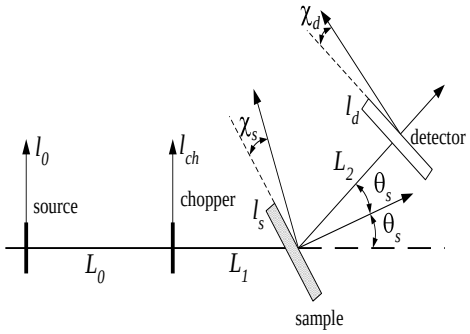

Figure 5

2.3.2. Steady State Source

For this geometry, (see Figure 5), following the above-described procedure, tacking account that in this case t_0 is the moment when the neutron reaches the chopper centre, $L = L_1 + L_2$,

$\Delta L = l_d \cdot \sin\chi_d - 2 \cdot l_s \cdot \cos\chi_d \cdot \sin\theta$, that the constraint introduced by the chopper presence is given by $t_0 = \gamma_2/\omega$, cancelling the "l_0", the "l_d" and "l_s" coefficients, one obtains respectively:

$$\left.\begin{aligned} \tan\theta_s &= -\frac{\pi m\omega}{hk}\cdot(L_1+L_2) \\ \tan\chi_d &= -\frac{L\cdot\tan\theta_s}{2\cdot L_2} \\ \tan\chi_d &= -\frac{L\cdot\tan\theta_s}{2\cdot L_2} \end{aligned}\right\} \qquad (13)$$

Three Axis Spectrometers

The experimental setup is given in Figure 6. As the real focusing effects are possible only when no Soller collimators are present between the spectrometer components this situation is considered below. Let us consider the idealized case of a neutron spectrometer with ideal perfect crystals and sample, monochromator and analyzer of negligible thickness.

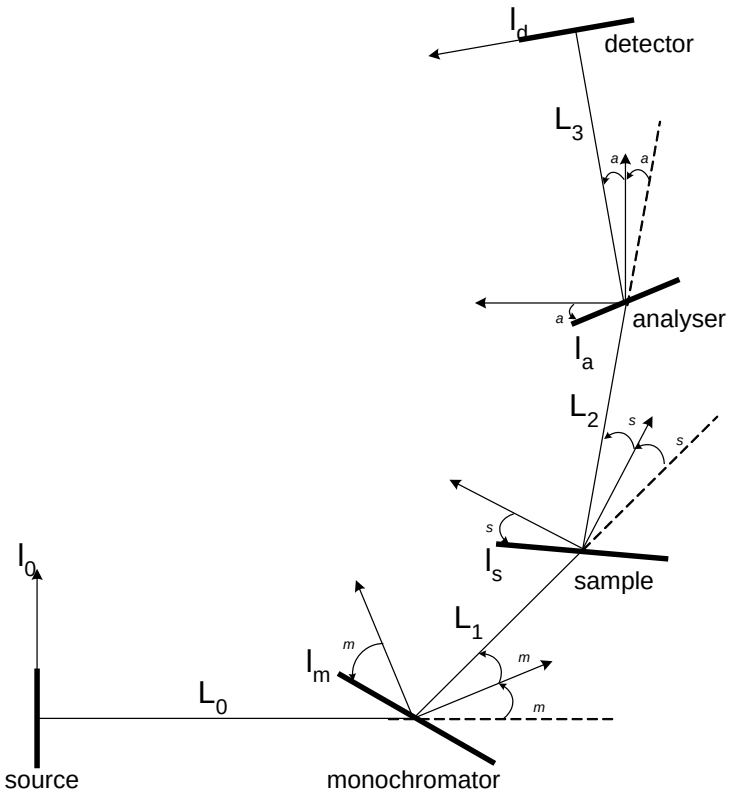

Figure 6

The spread of the scan variable can be written as a linear combinations between X vector components

$$\Delta = X_4 + C_1 \cdot X_1 + C_2 \cdot X_2 + C_3 \cdot X_3 \qquad (14)$$

where X is the vector of components ($Q\text{-}Q_0$, $\omega\text{-}\omega_0$), $Q = k_i - k_f$ and $h\omega = E_i - E_f$; k_i, k_f, E_i, E_f are the wave vectors respectively the energy for the incoming and the diffracted neutrons, while the "0" index refers to the corresponding most probable values. The X_1 and X_2 components are along respectively normal to Q_0 direction, all situated in the scattering plane. In the first approximation the X_3 component, normal to the scattering plane, should not be taken into consideration as there is no correlation

between horizontal and vertical variables. The variables defining the neutron trajectories in phase space are all the spatial relevant coordinates.
The expression giving the X components are:

$$X_1 = \cos\phi \cdot \Delta k_i + k_{i0} \cdot \sin\phi \cdot \gamma_i - \cos\phi' \cdot \Delta k \cdot -k_{f0} \cdot \sin\phi' \cdot \gamma_f \tag{15}$$

$$X_2 = -\sin\phi \cdot \Delta k_i + k_{i0} \cdot \cos\phi \cdot \gamma_i + \sin\phi' \cdot \Delta k_f - k_{f0} \cdot \cos\phi' \cdot \gamma_f \tag{16}$$

$$X_4 = \frac{h}{m} \cdot (k_{i0} \cdot \Delta k_i - k_{f0} \cdot \Delta k_f) \tag{17}$$

where

$$\left.\begin{aligned} \tan\phi &= \frac{k_{f0} \cdot \sin 2\theta_s}{k_{i0} - k_{f0} \cdot \cos 2\theta_s} \\ \varphi' &= \varphi - 2 \cdot \theta_s \end{aligned}\right\}, \tag{18}$$

and γ_i, γ_f are the horizontal divergence angles from the most probable trajectories, Δk_i, Δk_f are the corresponding wave vector spread, $2\theta_s$ is the scattering angle; the index i, f refers to the incoming respectively scattered neutrons; φ is the angle between Q_0 and k_{i0}.
To these relations must be added the Bragg constraints related to the monochromator and analyzer respectively:

$$\left.\begin{aligned} \gamma_0 + \gamma_1 &= 2 \cdot l_m \cdot \rho_m \\ \frac{\Delta k_i}{k_{i0}} &= \frac{\gamma_0 - \gamma_1}{2} \cdot \cot\theta_m \\ \gamma_2 + \gamma_3 &= 2 \cdot l_a \cdot \rho_a \\ \frac{\Delta k_f}{k_{f0}} &= \frac{\gamma_2 - \gamma_3}{2} \cdot \cot\theta_a \end{aligned}\right\} \tag{19}$$

where $\rho_m = 1/R_m$, $\rho_a = 1/R_a$ and R_m, R_a are the radius of curvature for the monochromator and analyzer respectively.
The geometry of the experimental configuration gives the following expressions for γ_0, γ_1, γ_3, γ_4:

$$\left.\begin{aligned} L_0 \cdot \gamma_0 &= -l_0 + l_m \cdot \sin(\theta_m + \chi_m) \\ L_1 \cdot \gamma_1 &= l_s \cdot \cos(\theta_s + \chi_s) + l_m \cdot \sin(\theta_m - \chi_m) \\ L_2 \cdot \gamma_2 &= -l_s \cdot \cos(\theta_s - \chi_s) + l_a \cdot \sin(\theta_a + \chi_a) \\ L_3 \cdot \gamma_3 &= l_d + l_a \cdot \sin(\theta_a - \chi_a) \end{aligned}\right\} \tag{20}$$

The angles χ_m, χ_a, all measured in trigonometric sense, represent the angle between to the lattice plane and the normal to the crystal surface, for monochromator and analyzer respectively.
Eliminating the angular variables γ_0 and γ_3 one obtains the following expressions for Δk_i, Δk_f:

$$\left.\begin{aligned} \Delta k_i &= k_{i0} \cdot \cot\theta_m \cdot (l_m \cdot \rho_m - \gamma_1) \\ \Delta k_f &= k_{f0} \cdot \cot\theta_a \cdot (l_a \cdot \rho_a - \gamma_2) \end{aligned}\right\} \tag{21}$$

Using (15), (16), (17) in (14) on obtains for the scan variable Δ:

$$\Delta = \Delta k_i \cdot A_i - A_f \cdot \Delta k_f + k_{i0} \cdot B_i \cdot \gamma_1 - k_{f0} \cdot B_f \cdot \gamma_2 \tag{22}$$

where:

$$\left.\begin{aligned} A_i &= k_{i0}\cdot\frac{h}{m}+C_1\cdot\cos\phi-C_2\cdot\sin\phi \\ A_f &= k_{f0}\cdot\frac{h}{m}+C_1\cdot\cos\phi'-C_2\cdot\sin\phi' \\ B_i &= C_1\cdot\sin\phi+C_2\cdot\cos\phi \\ B_f &= C_1\cdot\sin\phi'+C_2\cdot\cos\phi' \end{aligned}\right\} \tag{23}$$

Using (19) and (20) the relation giving the scan variable Δ becomes:

$$\begin{aligned}\Delta = k_{i0}\cdot l_m\cdot[\cot\theta_m\cdot\rho_m\cdot A_i+D_i\cdot\frac{\sin(\theta_m-\chi_m)}{L_1}]+l_s\cdot[D_i\cdot k_{i0}\cdot\frac{\cos(\theta_s+\chi_s)}{L_1}- \\ -D_f\cdot k_{f0}\cdot\frac{\cos(\theta_s-\chi_s)}{L_2}]+k_{f0}\cdot l_a\cdot[\frac{\sin(\theta_a+\chi_a)}{L_2}-\cot\theta_a\cdot\rho_a\cdot A_f]\end{aligned} \tag{24}$$

with

$$D_i = B_i - A_i\cdot\cot\theta_m \qquad D_f = -(B_f + A_f\cdot\cot\theta_a) \tag{25}$$

Cancelling the coefficients of l_m, l_a and l_s one obtains:

$$\frac{L_1}{2\cdot f_1}=1-\frac{B_i}{A_i}\cdot\tan\theta_m \qquad \frac{L_2}{2\cdot f_2}=1+\frac{B_f}{A_f}\cdot\tan\theta_a \tag{26}$$

$$\frac{\cos(\theta_s+\chi_s)}{\cos(\theta_s-\chi_s)}=\frac{L_1\cdot k_{f0}}{L_2\cdot k_{i0}}\cdot\frac{A_f\cdot\cot\theta_a+B_f}{A_i\cdot\cot\theta_m-B_i} \tag{27}$$

with:

$$f_1=\frac{\sin(\theta_m-\chi_m)}{2\cdot\rho_m} \qquad f_2=\frac{\sin(\theta_a+\chi_a)}{2\cdot\rho_a} \tag{28}$$

The first two conditions can be fulfilled by properly choosing the radius of curvature R_m, R_a for monochromator and analyzer respectively when varying k_i and k_f if L_1 and L_2 are fixed while the third one can be fulfilled by a proper sample orientation. The focusing conditions given by (26) assure the compensation of the contributions given by monochromator and analyzer respectively to the line width while the focusing condition (27) assures the sample contribution compensation.
The focusing conditions deduced above for an idealized configuration can serve as a "0"-th order approximation in a numerical optimization process.

Conclusions

Very high resolution performances can be obtained through inverse-space focusing in thermal neutrons spectrometry if focusing conditions involving monochromator and analysis radius of curvature and the sample orientation are fulfilled.
For time-of-flight instruments the inverse space focusing conditions given in [5] should be considered.
Inverse space focusing represents a very promising way to get high-resolution instruments in neutron spectrometry. A new concept of high-resolution instrument based on inverse space focusing effects could be developed.

This work was partially supported by IAEA Vienna under the contract 16049/RO.

References

[1] P. Boni 1996 *J. Neutron Research* **5**, 63
[2] M. Popovici, A. D. Stoica and I. Ionita 1987 *J.Appl. Cryst.* **20**, 90
[3] I. Ionita, A. D. Stoica, M. Popovici, N. C. Popa 1999 *Nucl. Instr. & Meth. in Physics Research*

A431 509-520
[4] I. Ionita, A. D. Stoica 2000 The Crystal Neutron Diffractometer Resolution Function Spatial Effects Included, *J. Applied Cryst.* **33**, 1067
[5] I. Ionita 2002 Focusing Conditions in Neutron Spectrometry, *Nucl. Instr.& Meth. in Physics Research* 313-336.